Received: 6 November 2019 | Revised: 24 December 2020 | Accepted: 3 January 2021

DOI: 10.1111/ede.12372

RESEARCH

WILEY

Tergal and pleural wing-related tissues in the German cockroach and their implication to the evolutionary origin of insect wings

Courtney Clark-Hachtel[1] | **Ana Fernandez-Nicolas**[2] | **Xavier Belles**[2] | **Yoshinori Tomoyasu**[1]

[1]Department of Biology, Miami University, Oxford, Ohio, USA

[2]Institute of Evolutionary Biology, CSIC-Universitat Pompeu Fabra, Barcelona, Spain

Correspondence
Yoshinori Tomoyasu, Department of Biology, Miami University, 700E High St, Pearson Hall, Oxford, Ohio, 45056, USA.
Email: tomoyay@miamioh.edu

Present address
Courtney Clark-Hachtel, Department of Biology, University of North Carolina at Chapel Hill, Chapel Hill, NC.

Ana Fernandez-Nicolas, Department of Molecular Biology, Cell Biology and Biochemistry, Brown University, Providence, Rhode, Island.

Funding information
Division of Integrative Organismal Systems, Grant/Award Number: IOS1557936; European Fund for Economic and Regional Development; Catalan Government, Grant/Award Numbers: 2017 SGR 10c0, 2014 SGR 619; Division of Graduate Education, Grant/Award Number: GRFP; Miami University Faculty Research Grants Program; Spanish Ministry of Economy and Competitiveness, Grant/Award Numbers: CGL2012-36251, CGL2015-64727-P, PID2019-104483GB-I00

Abstract

The acquisition of wings has facilitated the massive evolutionary success of pterygotes (winged insects), which now make up nearly three-quarters of described metazoans. However, our understanding of how this crucial structure has evolved remains quite elusive. Historically, two ideas have dominated in the wing origin debate, one placing the origin in the dorsal body wall (tergum) and the other in the lateral pleural plates and the branching structures associated with these plates. Through studying wing-related tissues in the wingless segments (such as wing serial homologs) of the beetle, *Tribolium castaneum*, we obtained several crucial pieces of evidence that support a third idea, the dual origin hypothesis, which proposes that wings evolved from a combination of tergal and pleural tissues. Here, we extended our analysis outside of the beetle lineage and sought to identify wing-related tissues from the wingless segments of the cockroach, *Blattella germanica*. Through detailed functional and expression analyses for a critical wing gene, *vestigial* (*vg*), along with re-evaluating the homeotic transformation of a wingless segment induced by an improved RNA interference protocol, we demonstrate that *B. germanica* possesses two distinct tissues in their wingless segments, one with tergal and one with pleural nature, that might be evolutionarily related to wings. This outcome appears to parallel the reports from other insects, which may further support a dual origin of insect wings. However, we also identified a *vg*-independent tissue that contributes to wing formation upon homeotic transformation, as well as *vg*-dependent tissues that do not appear to participate in wing formation, in *B. germanica*, indicating a more complex evolutionary history of the tissues that contributed to the emergence of insect wings.

KEYWORDS
Blattella germanica, evolutionary origin, Hox, insect wings, morphological novelty, serial homology, *vestigial*

1 | INTRODUCTION

The debate surrounding the evolutionary origin of the insect wing has been ongoing for over 200 years (Clark-Hachtel & Tomoyasu, 2016). Over the course of this debate, extensive investigations from various fields have resulted in two prominent hypotheses on the origin of insect wings (reviewed in Clark-Hachtel & Tomoyasu, 2016; Quartau, 1986). The first hypothesis connects the origin of insect wings to lateral outgrowths of the dorsal body wall (tergal origin; e.g., see Rasnitsyn, 1981). The second hypothesis proposes that insect wings arose from ancestral proximal leg components (pleural origin; e.g., see Kukalova-Peck, 1983). These two hypotheses have historically been in opposition with one another, with neither hypothesis able to surpass the other. Recently, a third hypothesis, the dual origin hypothesis, has come to light. This hypothesis proposes that both tergal and pleural tissues contributed to the evolution of insect wings and thus resolves some of the conflicts between the two previously competing hypotheses (Clark-Hachtel & Tomoyasu, 2016; Rasnitsyn, 1981; Tomoyasu, 2018). Support for this third hypothesis has come from the identification of wing-related tissues (wing serial homologs, wing homologs, and other tissues whose development relies on wing genes) in non-winged segments of insects and other arthropods (Clark-Hachtel & Tomoyasu, 2020; Clark-Hachtel et al., 2013, 2018; Elias-Neto & Belles, 2016; Linz & Tomoyasu, 2018; Mashimo & Machida, 2017; Medved et al., 2015; Requena et al., 2017), as well as from detailed paleontological analyses (Prokop et al., 2017).

In insects, only the second and third thoracic segments (T2 and T3, respectively) possess wings, while the first thoracic segment (T1) and the abdominal segments are wingless. The identification of the tissues that share an evolutionary origin with wings in wingless segments (i.e., wing serial homologs) can be a powerful approach to gain insight into how the insect wing originated, as the variation in type and degree of modification imposed upon wing serial homologs can provide us with a snapshot of different evolutionary states for tissues related to insect wings. Historically, structures serially homologous to wings have been identified mainly through their morphological similarity to wings (Tomoyasu et al., 2017). However, among the wing serial homologs, the insect wing appears to have undergone the most extensive evolutionary modifications (i.e., the insect wing represents the most apomorphic condition; Tomoyasu et al., 2017), making it difficult to comprehensively identify wing serial homologs outside of the winged segments based on morphological similarity with wings. Recently, the field of evolutionary and developmental biology (evo-devo) has facilitated the identification of wing serial homologs in wingless segments through (i) identifying tissues outside of the winged segments that share gene expression and functional dependency with wings and (ii) analyzing the ability of tissues in wingless segments to contribute to ectopic wings upon the transformation of wingless segments into winged segments via manipulation of Hox genes (regional selector genes; Tomoyasu et al., 2017).

The first approach has been applied to various insects, as well as to the identification of wing homologs from some noninsect arthropods, providing important insight into the evolutionary origin of insect wings (Averof & Cohen, 1997; Clark-Hachtel & Tomoyasu, 2020; Clark-Hachtel et al., 2013; Elias-Neto & Belles, 2016; Hrycaj et al., 2010; Hu et al., 2018; Linz & Tomoyasu, 2018; Medved et al., 2015; Niwa et al., 2010; Ohde et al., 2013). One gene that has been used extensively in these studies is *vestigial* (*vg*; Clark-Hachtel & Tomoyasu, 2016, 2020; Clark-Hachtel et al., 2013; Linz & Tomoyasu, 2018; Niwa et al., 2010; Ohde et al., 2013; Tomoyasu et al., 2017). *vg* is considered a critical wing gene because of its essential function during wing development (Halder et al., 1998; Williams et al., 1991) and its ability to induce ectopic wing tissues in certain contexts when overexpressed (Baena-López & García-Bellido, 2003; Kim et al., 1996). The identification of *vg*-dependent tissues has been crucial in revealing wing serial homologs in beetles (Clark-Hachtel et al., 2013; Linz & Tomoyasu, 2018; Ohde et al., 2013), and more recently, in identifying tissues that are potentially homologous to insect wings (i.e., wing homologs) from a crustacean, *Parhyale hawaiensis* (Clark-Hachtel & Tomoyasu, 2020). The second approach, Hox manipulation, has also been informative to uncover the evolutionary origin of insect wings. Hox genes are regional selector genes responsible for the individualization and differentiation of each segment in insects (Angelini & Kaufman, 2005; Hughes & Kaufman, 2002; Pearson et al., 2005). Hox genes achieve this function through differential modification of serially homologous structures. Therefore, removing Hox function can allow us to strip away these modifications and reveal serial homologs that would otherwise be difficult to recognize through morphological analysis alone (e.g., see Sánchez-Higueras et al., 2014, in which the authors revealed the serial homology of two functionally and morphologically very distinct tissues, trachea and endocrine organs through, in part, modifying Hox function). Previous studies have identified wing serial homologs in T1 of several insects through investigating tissues that contribute to the formation of ectopic wings when *Sex combs reduced* (*Scr*), the T1 Hox gene, is knocked down (Clark-Hachtel et al., 2013, 2018; Elias-Neto & Belles, 2016; Hrycaj et al., 2010;

Medved et al., 2015; Rogers et al., 1997). Using these two approaches, wing (serial) homologs have now been identified in a breadth of species representing multiple branches of the arthropod phylogeny, from crustaceans to holometabolous winged insects (Averof & Cohen, 1997; Clark-Hachtel & Tomoyasu, 2020; Clark-Hachtel et al., 2013, 2018; Elias-Neto & Belles, 2016; Hrycaj et al., 2010; Linz & Tomoyasu, 2018; Medved et al., 2015; Niwa et al., 2010; Ohde et al., 2013; Tomoyasu et al., 2017, also reviewed in Clark-Hachtel & Tomoyasu, 2016; Tomoyasu et al., 2017).

As polyneopterans with hemimetabolous development, cockroaches occupy an informative position on the arthropod phylogeny, where they can provide us with a snapshot of the state of wing serial homologs between non-winged arthropods and holometabolous insects, which can give us a better understanding of the evolutionary history of wing-related tissues. The idea of exploiting the unique phylogenetic position of cockroaches to gain insight into the insect wing origin is not new. As early as 1964, a homeotic mutant of the German cockroach, *Blattella germanica*, was identified and described (Ross, 1964). This mutant, named *Prowing*, possessed ectopic wings on T1 that appear to develop from the lateral edge of the dorsal tergum, leading the author to view this as evidence in support of a tergal origin of insect wings (Ross, 1964). More recently, Hrycaj et al. (2010) knocked down *Scr* via RNA interference (RNAi) in the American cockroach, *Periplaneta americana*, and found that reduction of *Scr* during later stages of development led to the production of ectopic wings on T1. Similar to what was seen in the *Prowing* mutants of *B. germanica*, the ectopic wings formed from *Scr* knockdown in *P. americana* appear to be primarily of lateral dorsal tergal origin. Therefore, these authors also concluded that this provided further evidence for a tergal origin of insect wings (Hrycaj et al., 2010). Through detailed analysis of the tissues that contribute to T1 wing upon *Scr* RNAi in *B. germanica*, Elias-Neto and Belles (2016) confirmed that the tergal edge of *B. germanica* T1 contributes to ectopic wing. In addition, they identified a region of the pleuron that also contributes to the formation of ectopic T1 wing in *B. germanica*. This finding of two distinct regions, one of tergal identity and one of pleural, that contribute to ectopic wing in T1, led the authors to propose that both of these structures are wing serial homologs in the wingless T1 segment and provided further evidence in support of a dual origin of insect wings (Elias-Neto & Belles, 2016).

The studies mentioned above have been helpful in advancing our understanding of the possible wing serial homologs in cockroaches. These studies mainly utilized homeotic transformation to identify possible wing serial homologs (the above mentioned second approach). To complement and expand upon the knowledge of wing serial homologs obtained from these previous cockroach studies, in this study, we took the above mentioned first approach by investigating the function of *vg* during *B. germanica* development and identifying *vg*-dependent tissues in the wingless segments of this species. In addition, while seeking a way to maximize the effect of *vg* RNAi, we were able to establish an improved injection scheme for post-embryonic gene knockdown in *B. germanica*. We took advantage of this revised protocol and revisited the T1 transformation induced by *Scr* knockdown to see if we could obtain further information about the T1 wing serial homologs. Through these analyses, we found that *B. germanica* possesses two distinct tissues in their wingless segments, one tergal and one pleural, that might be evolutionarily related to wings. This outcome appears to parallel reports in the wingless segments of other insects, which may further support a dual origin of insect wings. However, our study also revealed two intriguing aspects of *vg*-dependent tissues in *B. germanica*, which may require a revision of the "two sets of *vg*-dependent wing serial homologs per segment" view that was initially observed in *Tribolium castaneum* (Clark-Hachtel et al., 2013; Linz & Tomoyasu, 2018). First, the pleural structures that contribute to ectopic T1 wing upon homeotic transformation appear to be independent of *vg*, at least during nymphal development. Second, some *vg*-dependent structures may not be wing serial homologs and may, instead, represent the ancestral function of *vg* in arthropods before wings evolved, such as functioning to pattern posterior tergal edge (Clark-Hachtel & Tomoyasu, 2020). These discrepancies between the wing serial homologs and *vg*-dependent tissues in *B. germanica* (even though these two categories of tissues still largely overlap) are likely a reflection of a complex evolutionary history of the tissues that contributed to the formation of insect wings, demanding further investigation to gain a comprehensive understanding of how the insect wing, a morphologically highly novel and ecologically critical structure, evolved.

2 | MATERIALS AND METHODS

2.1 | Cockroach culturing and mutant specimen

B. germanica cultures were obtained from Carolina Biological. This culture was inbred to produce the laboratory strain used for experiments. All *B. germanica* cultures were reared in the dark at 30°C with mouse chow (LabDiet, rodent diet 5010) and water ad libitum.

Ethanol preserved specimens of the *Prowing* mutant were obtained from Dr. Donald Mullins at Virginia Tech.

2.2 | Gene cloning and dsRNA synthesis

The *B. germanica* orthologs of *vg* (*Bg-vg*) and *Scr* (*Bg-Scr*) were identified by BLAST against a de novo assembled transcriptome (sixth instar nymph) using the corresponding *Drosophila melanogaster* proteins as queries. Fragments of these genes were amplified from *B. germanica* cDNA made from RNA isolated from sixth instar nymphs and cloned into a pCR4-TOPO vector (pCR4-TOPO-TA Cloning Kit, Thermo Fisher Scientific). The primers used in this study are listed in Table S1. Double-stranded RNA (dsRNA) for injection was prepared as previously described (Philip & Tomoyasu, 2011) using the primers listed in Table S1. The sequences of *Bg-vg* and *Bg-Scr* are available on GenBank (accession numbers MN337883 and MN337884).

2.3 | Cockroach injection and RNAi off-target assessment

Three different injection schemes were used in this study: (i) injection of dsRNA 7 days post-hatching (dph, corresponding to late first or early second instar nymph) and killed as adults for analysis (red box, Figure S1), (ii) injection 14 dph (corresponding to late third or early fourth instar nymph), reinjected 21 dph and 27 dph and killed as adults for analysis (blue box, Figure S1) and (iii) injection 21 dph (corresponding to late fourth or early fifth instar nymphs), reinjected 27 dph and killed as adults for analysis (purple box, Figure S1). With each scheme, cockroaches were injected in the ventral abdomen with ~1 μl of 1 μg/μl dsRNA for the gene of interest using a 10 μl Hamilton microsyringe, except for 7 dph injections, which were injected with 0.5–0.7 μl of 1 μg/μl dsRNA using a microinjector (Linz et al., 2014; Philip & Tomoyasu, 2011). dsRNA for *Enhanced Yellow Fluorescent Protein* (*EYFP*; see primer information in Table S1) was injected as a negative control into age-matched groups for each injection scheme. The injection scheme that produced the most severe RNAi phenotypes across traits scored (see below) was scheme (ii) (blue box in Figure S1; Tables 1 and S2). Although this scheme also showed a slight delay in development compared to scheme (iii) (Figure S3), this delay was likely due to injection alone, as ds*EYFP* injected cockroaches were also delayed compared to uninjected controls (Figure S3). For *Bg-Scr* RNAi, only scheme (ii) was used. The absence of off-target effect was confirmed when RNAi for two nonoverlapping regions of the gene of interest (either *Bg-vg* or *Bg-Scr*) produced the same phenotypes (see Figure S4 for phenotypes of the *Bg-Scr* off-target fragment). The detailed primer information for these nonoverlapping fragments can be seen in Table S1 and phenotype information for *Bg-vg* RNAi nonoverlapping fragments can be found in Figure S2, and Tables 1 and S2.

2.4 | Embryo collection and in situ hybridization

Adult female *B. germanica* for embryo collection were isolated on the day that they extruded their ootheca (egg case; ootheca Day 0, ODO). These females were then aged with their ootheca until the embryos were in the desired stage. For this study, oothecae were killed on Day 3 (OD3), Day 4 (OD4), and Day 5 (OD5), for embryo fixation. To fix embryos for in situ hybridization, the egg cases were gently removed from the female and placed in PBT in a microcentrifuge tube. To isolate the embryos, the oothecae were boiled at 100°C for 10 min and dissected in 8% Formaldehyde/PBT with 1% EGTA. Embryos were then fixed in this solution for 1 h at room temperature, washed with 100% methanol, and stored at −20°C at least overnight before staining.

In situ hybridization was performed following a modified version of a previously published protocol (Shippy et al., 2009; Tomoyasu et al., 2009). Briefly, the *Bg-vg* riboprobe template was prepared from the cDNA fragment cloned in pCR4-TOPO via restriction digestion (NotI). The antisense riboprobe was synthesized with T3 polymerase and purified via ethanol precipitation. Before rehydration, embryos were treated with 1:1 (v/v) xylene:ethanol (a procedure adapted from Nagaso et al., 2001). After rehydration embryos were permeabilized with 80% acetone at −20°C for 10 min and then post-fixed in 8% formaldehyde/PBS for 20 min at room temperature (also adapted from Nagaso et al., 2001). The remaining steps of in situ hybridization followed the previously published protocol (Shippy et al., 2009; Tomoyasu et al., 2009), with the exception of the use of a ratio of 3:2000 riboprobe:hybridization buffer for hybridization and longer washes immediately following hybridization (two 3-h washes). Embryos were stained using Fast Red (Sigma F4648) for fluorescent imaging. The complete in situ hybridization protocol for *B. germanica* embryos is provided as a supplemental material (Supporting Information Doc 1).

TABLE 1 Frequency and scores of *Bg-vg* RNAi-related traits in various injection schemes and treatments. Possible max score for each category is indicated in parentheses

	Traits with RNAi phenotype															
	Wing		T1 posterior edge		T1 dorsal pigmentation		T2 and T3 scutellum		Lateral abdominal tergum		A9		Abdominal pleuron		Lateral abdominal sternum	
	%	Score (30)	%	Score (10)	%	Score (10)	%	Score (20)	%	Score (10)	%	Score (10)	%	Score (20)	%	Score (10)
Bg-vg F2R2 scheme (ii)	100	30	100	10	100	10	100	20	70	7	100	10	70	14	80	8
Bg-vg F2R2 scheme (iii)	97	29	80	8	100	10	100	20	20	2	100	10	65	13	30	3
Bg-vg F1R1 scheme (ii)	40	12	20	2	100	10	65	13	30	3	90	9	45	9	0	0
Bg-vg F2R2 scheme (i)	17	5	30	3	50	5	35	7	20	2	40	4	50	10	10	1
EYFP 400 bp scheme (ii) & (iii)	0	0	0	0	10	1	30	6	0	0	80	8	15	3	0	0
Uninjected Control scheme (ii) & (iii)	0	0	0	0	0	0	20	4	0	0	30	3	10	2	0	0

2.5 | *vestigial* RNAi phenotype scoring

Ten adult females were selected at random from each injection scheme and treatment combination. For ds*EYFP* injected and uninjected control, 10 adult females were selected from scheme (ii) and (iii) combined, as there was no phenotypic difference between injection schemes in these groups. As cockroaches are sexually dimorphic, females were used for all analyses. However, the presence of *Bg-vg* RNAi (and *Bg-Scr* RNAi) phenotypes was confirmed in males for each trait (Figures S5 and S6). Each *Bg-vg* RNAi-related trait was scored as 0 (trait not observed) or 1 (trait observed), except for the wing, T2 and T3 scutellum, and the abdominal pleuron (Table S2). The wing was scored as 0 (trait not observed), 1 (mild reduction), 2 (moderate reduction), and 3 (severe reduction; Table S2). The T2 and T3 scutellum and abdominal pleuron were scored as 0 (no defect), 1 (reduced), and 2 (missing) (Table S2). The total score from 10 individuals was then divided by the possible max score of each trait to obtain the frequency of RNAi phenotypes for all traits in each injection scheme and treatment combination (Table 1 and Figure S2).

2.6 | Documentation and image processing

Adult cockroaches were fixed in 4% formaldehyde in 0.1 M phosphate buffer (pH = 7.3) overnight at 4°C and stored in 70% EM-grade ethanol before documentation (modified from Elias-Neto & Belles, 2016). The T1 segment was dissected from some cockroaches for documentation (*Bg-Scr* RNAi and wild-type). Whole adults and dissected T1 were imaged using a Zeiss AxioCam MRc5 or a Zeiss Axiocam 503 color camera (males and late instar nymph) with Zeiss Discovery V12. Zeiss AxioVison Extended Focus module was used to obtain images with increased focus depth. Fast Red stained embryos were mounted in 80% glycerol and imaged on a Zeiss LSM 710 Confocal Microscope. Images were adjusted for contrast and brightness only, using Adobe Photoshop CC. Imaris (Bitplane) was used to create the 3D rendering for Supporting Information Movie S3.

3 | RESULTS

3.1 | *vestigial* expression pattern in the *Blattella germanica* embryo

To identify *vg*-dependent tissues from *B. germanica*, we first investigated the expression pattern of *Bg-vg* during early embryo development using in situ hybridization (Figure 1). *B. germanica* embryogenesis takes about 20 days (Maestro et al., 2010; Piulachs et al., 2010). The earliest onset of *Bg-vg* expression can be seen in the brain on Day 3 of development (white circle in Figure 1a). By Day 4 of embryonic development, *Bg-vg* expression becomes apparent in the epidermis, and by Day 5 of development, this expression becomes more pronounced (Figure 1b–d). On Day 4 and Day 5, *Bg-vg* is expressed segmentally at the edge of the dorsal terga throughout the thorax and abdomen (arrow in Figure 1b–d). This tergal expression of *Bg-vg* encompasses the lateral and posterior edge of the terga, forming an L-shaped expression pattern. In T1, a U-shaped tergal expression pattern is formed from the expansion of the tergal expression of *Bg-vg* into the anterior edge of this segment. This *vg* expression pattern ("U-shaped" expression in T1 and "L-shaped" expression in the thoracic and abdominal segments posterior to T1) appears to be conserved across various orders of insects (Clark-Hachtel et al., 2013; Niwa et al., 2010), as well as in a crustacean (Clark-Hachtel & Tomoyasu, 2020). By Day 5 of development, *Bg-vg* expression can also be observed in the ventral nerve cord (Figure 1e–e′; Supporting Information Movie S1).

In all three thoracic segments, *Bg-vg* is also expressed in the proximal portion of the leg (* Figure 1b–d,f,g). This *Bg-vg*-expressing tissue appears to be mesodermal, as it is entirely encased within the leg epidermis (Figure 1f,g; Supporting Information Movies S2 and S3). *vg* has been shown to be important for proper muscle development in *D. melanogaster* (Bernard et al., 2003; Deng et al., 2009, 2010), therefore it is likely that this *Bg-vg* expression in the proximal leg mesoderm corresponds to future muscle tissue (Figure 1f,g). It is also worth mentioning that this *vg*-positive mesodermal cell population in *B. germanica* appears to correspond to the second *vg*-positive tissue in the *T. castaneum* embryos that we previously speculated to be pleural-related *vg*-positive tissues (Clark-Hachtel et al., 2013). We are currently re-evaluating *vg* expression in detail in *T. castaneum*.

Upon detailed analysis of *Bg-vg* expression in the thorax, we also noticed another cluster of *Bg-vg* positive cells positioned between the tergal epidermal *Bg-vg* expressing cells and the presumptive *Bg-vg* positive muscle cells (+ in Figure 1g′; Supporting Information Movies S2 and S3). This cluster of *Bg-vg* positive cells appears to be connected to the tergal *Bg-vg* expression domain but is ventral to the spiracle (Figure 1g–g′; Supporting Information Movies S2 and S3), a landmark that is often used to delineate the boundary between tergal and pleural tissues (Mashimo & Machida, 2017). Therefore, these ventrally located *Bg-vg* positive cells might correspond to the thoracic pleuron of *B. germanica*, although it is also

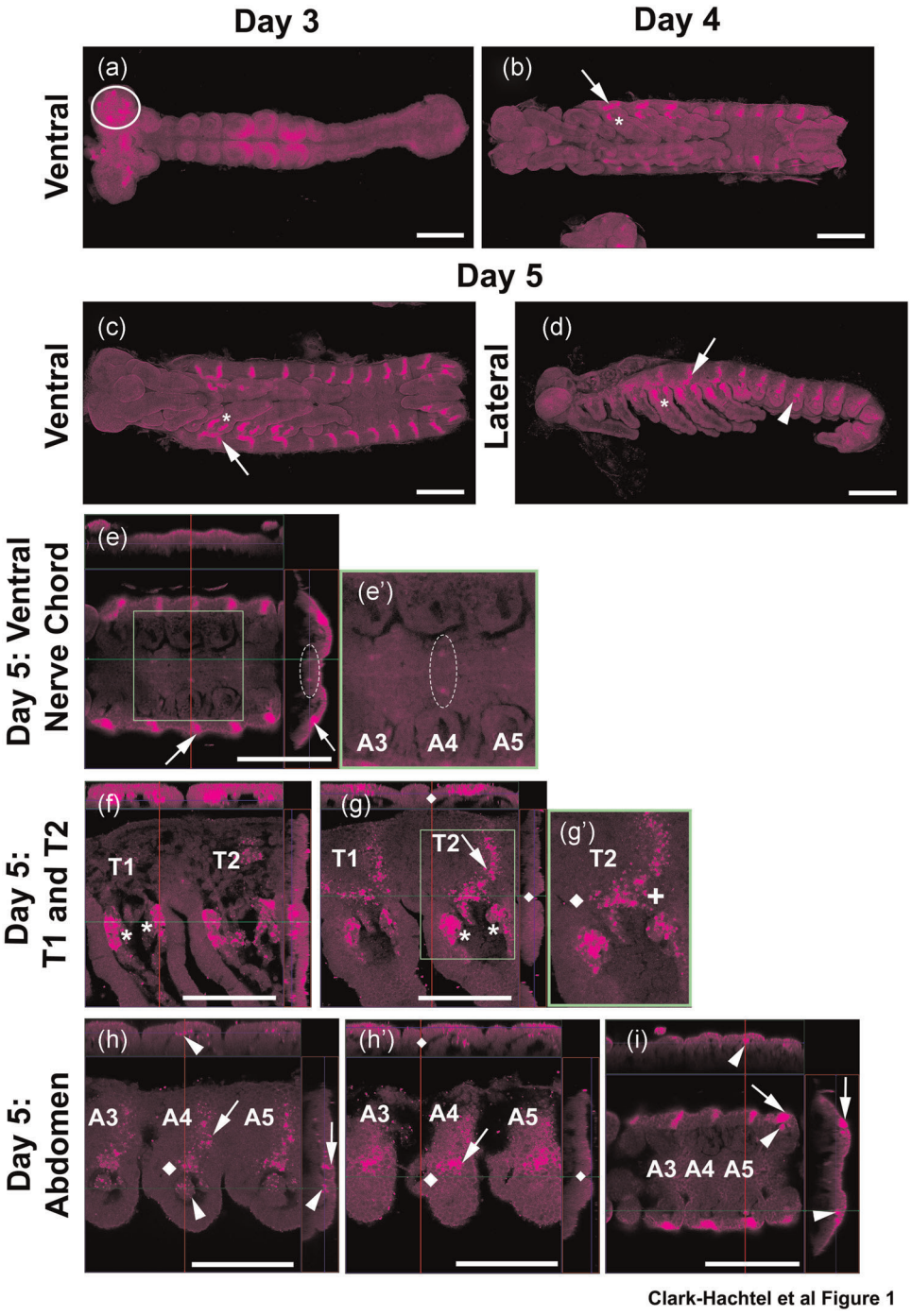

FIGURE 1 *Bg-vg* expression in the *Blattella germanica* embryo. (a–d) Overall *Bg-vg* expression in *B. germanica* embryos at Day 3 (a), Day 4 (b), and Day 5 (c, d) of development. (e–i) Detailed *Bg-vg* expression on day 5 of development. Side panels correspond to area outlined by green box. (e–e, g–g′) Ventral view of *Bg-vg* expression in the ventral nerve cord of *B. germanica* (dashed oval). (f–g′) Lateral view of *Bg-vg* expression in T1 and T2. + indicates possible pleural population of *Bg-vg* positive cells. (h–h′) lateral and (i) ventral views of *Bg-vg* expression in the abdomen. Indicators are as follows: white circle (early expression in brain), arrow (tergal expression), + (possible pleural expression). * (proximal leg muscle precursor expression), arrowhead (expression in ventral region of the abdomen), ♦ (spiracle). Scale bars in a–d are 200 μm and scalebars in e–i are 100 μm [Color figure can be viewed at wileyonlinelibrary.com]

possible that they are mesodermal. Further study will be required to determine the nature of these *Bg-vg* positive cells. We also found an additional population of *Bg-vg* positive cells outside of the terga in the abdominal segments (arrowhead in Figure 1d,h,i). These *Bg-vg* positive cells are ventral to the spiracle and completely internalized but remain in contact with the epidermis (-Figure 1h,i; Supporting Information Movies S1 and S4). Similar to the situation in the thorax, the nature of this additional *Bg-vg* positive cell population, specifically whether it belongs to pleuron (ectoderm) or muscles (mesoderm), is currently elusive.

In summary, our expression analysis has revealed that *Bg-vg* is expressed in several distinct tissues of the embryo, including tergal edges, the nervous system, and the muscles located within the proximal leg. The additional *Bg-vg* expressing cell population located ventrally to the spiracle in the thorax and abdomen could be pleural or mesodermal, for which further studies will be required to determine their precise nature. Also, due to technical limitations of performing in situ hybridization at later stages of *B. germanica* embryogenesis, we were unable to obtain expression information for *Bg-vg* after Day 5. Considering that *B. germanica* embryos hatch at ~20 days after ootheca development, it is quite possible that there are additional *Bg-vg* expressing tissues and cells later in embryogenesis.

3.2 | *vestigial* is essential for wing and body wall development in *Blattella germanica*

We next performed RNAi for *Bg-vg* to identify the tissues that are functionally dependent on *vg* both in the winged and wingless segments. For our analysis of *Bg-vg* dependent tissues to be informative about possible wing serial homologs, it is crucial that *Bg-vg* function in wing development is evolutionarily conserved in *B. germanica*. We found this to be the case, as the most prominent *Bg-vg* RNAi phenotype we observed was the severe reduction of wings on T2 and T3 (Figures 2a,b, S2, S5a,b, and S7b; Table 1). This indicates that *vg* function in coordinating wing development is conserved, even in hemimetabolous insect lineages, such as cockroaches.

In addition to wing development, *Bg-vg* RNAi also affected the development of the tergal edge in cockroaches (Figures 2c–i′ and S5c–h′). The posterior T1 tergal edge of *Bg-vg* RNAi individuals is often reduced relative to wild-type (compare bracket in Figures 2c–c′ to d–e′, S2, and S5c–c′ to d–d′; Tables 1 and S2). Additionally, the lateral tergal edge of T1 is reduced upon knockdown of *Bg-vg* (Figures 2c,e–g and S5e,f). The pigmentation on the dorsal surface of T1 also expands in *Bg-vg* RNAi individuals relative to wild-type (Figures 2c,d, S2, and S5c,d; Tables 1 and S2), although this trait might represent the maintenance of nymphal pigmentation, as late instar nymphs have similarly expanded dorsal pigmentation (Figure S7g). The *Bg-vg* dependency of the tergal edge is not limited to T1. We noticed a shape change in the edge of the abdominal tergum upon *Bg-vg* RNAi, demonstrating that the edge of the abdominal tergum, both lateral and posterior, is also *Bg-vg* dependent (white outline in Figures 2h′,i′, S2, and S5g′,h′; Tables 1 and S2). We observed a similar shape change in the posterior edge of the dorsal tergum of the ninth abdominal segment (A9, white outline in Figures S5o,p and S7e,f), although this shape change in A9 may not be specific to *Bg-vg* function, as it is also seen frequently in ds*EYFP* injected negative control (Tables 1 and S2; Figure S2). Interestingly, we also found that in T2 and T3, in addition to wing formation, *Bg-vg* RNAi affected the proper development of the posterior edge in these thoracic segments, specifically the formation of the scutellum (dorsal posterior body wall protrusion, * in Figures 2j–j′ and S5i–i′). Upon reduction of *Bg-vg*, the scutellum is often reduced or missing (Figures 2j–j′,k–k′, S2, S5i–i′,j–j′, and S7c–c′; Tables 1 and S2), indicating that the functional domain of *Bg-vg* (within ectoderm) is not limited to wings even in the winged segments.

In the abdomen, in addition to the *Bg-vg* dependent tergum, we also identified a plate that is dependent on *Bg-vg* (Figures 2h–h′ and S5k–k′). This plate is sclerotized and pigmented and can be considered part of the pleuron as it is located between the ventral sternum and dorsal tergum (Snodgrass, 1935a). Upon *Bg-vg* RNAi, this pleural plate is often reduced or even missing (Figures 2i–i′, S2, S5l–l′, and S7d–d′; Tables 1 and S2). We also noticed that the lateral edge of the abdominal sternum undergoes a shape change upon *Bg-vg* RNAi (white outline in Figures 2l–m′, S2, and S5m–n′; Tables 1 and S2). However, we failed to reproduce this sternum phenotype with a nonoverlapping fragment for *Bg-vg* (Tables 1 and S2; Figure S2), leaving the possibility that this shape change in sternum is due to off-target effects of the first *Bg-vg* dsRNA fragment. In contrast to the situation in the abdomen, we were unable to identify any effects of *Bg-vg* RNAi on the pleural tissues in the T1 segment of *B. germanica*, as the pleural T1 of *Bg-vg* RNAi individuals and wild-type look very similar (Figures 2f–g′ and S5e,f).

Taken together, our RNAi analysis for *Bg-vg* has revealed that *Bg-vg* is important for tergal edge development throughout the thorax, even in T2 and T3, and in the abdomen of *B. germanica*. This outcome is consistent

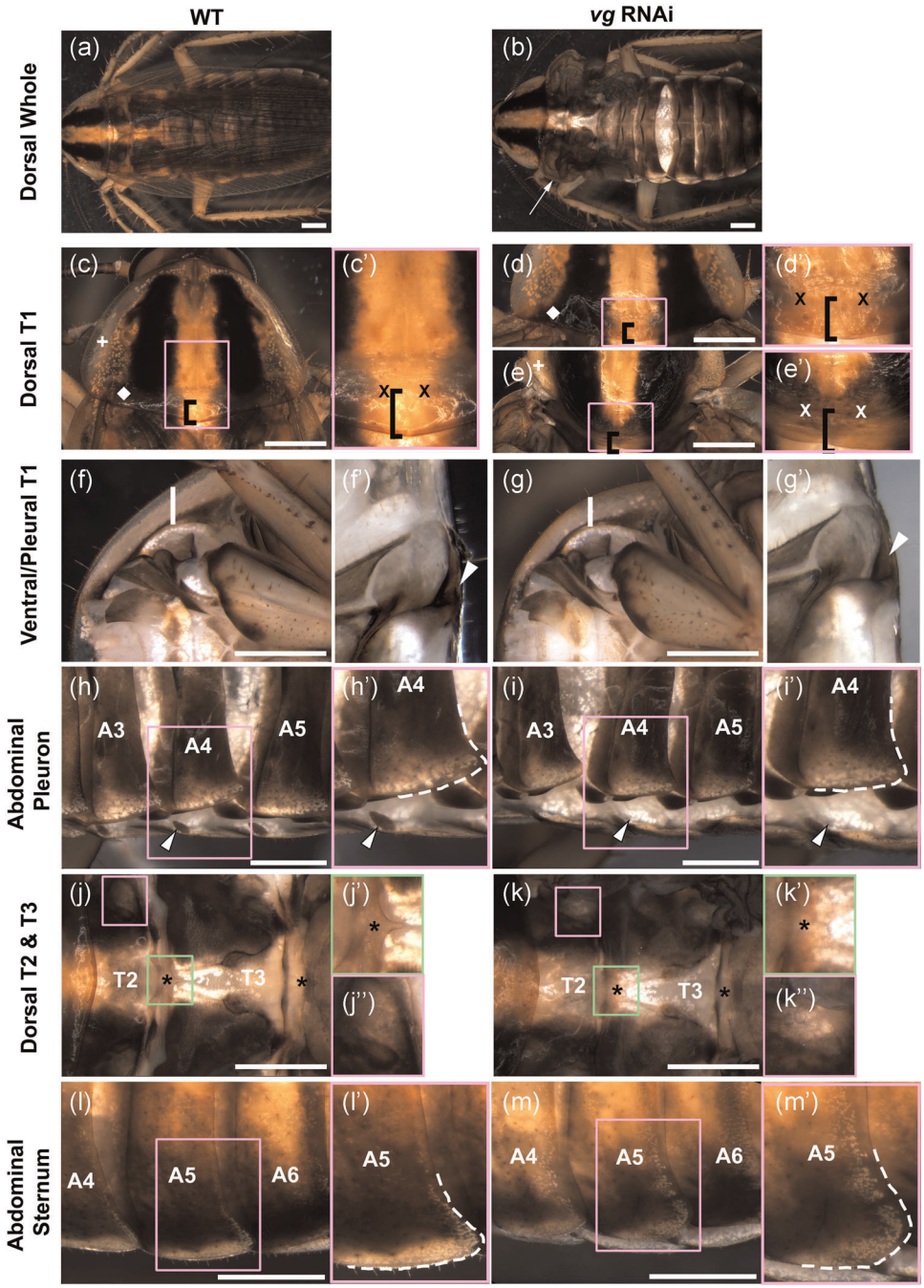

FIGURE 2 Effects of *Bg-vg* RNAi in the formation of wings, tergal edge, and pleuron in *Blattella germanica*. Wild-type (a, c–c′, f–f′, h–h′, j–j″, l–l′) and *Bg-vg* RNAi (b, d–e′, g–g′, i–i′, k–k″, m–m′) *B. germanica*. Side panels correspond to areas outlined by box of respective color, except f′ and g′ where side panels are a lateral view of the T1 pleuron of partially dissected animals (anterior is up). **X** in c′, d′, and e′ marks the corner of a semi-triangular landmark pigmentation used to determine the upper limit of the bracket to evaluate posterior reduction of T1 in *Bg-vg* RNAi individuals. Indicators are as follows: arrow (wing), + (dorsal lateral tergal edge), ◆ (dorsal T1 pigmentation), black bracket (posterior edge of the T1 tergum), white line (lateral edge of the T1 tergum), arrowhead (T1 pleural plate (f′ and g′) or abdominal *vg*-dependent pleural plate (h–j′)), dashed white outline (h′ and i′, lateral abdominal tergum and l′ and m′, lateral abdominal sternum, * (T2 and T3 scutellum). pink box in j and k (the T2 sensory patch). All scale bars are 1 mm [Color figure can be viewed at wileyonlinelibrary.com]

with the expression of *Bg-vg* in these areas of the embryo and corroborates the idea that the tergal edge of wingless segments is a wing serial homolog in *B. germanica*. Furthermore, we found that the formation of an abdominal pleural plate is dependent on *Bg-vg*, suggesting that there are two distinct wing serial homologs in *B. germanica*, at least in their abdominal segments. However, the absence of *vg*-dependent pleural plates in T1 of *B. germanica* presents a situation different from that of *T. castaneum* where there are both tergal and pleural *vg*-dependent T1 tissues (Clark-Hachtel et al., 2013).

3.3 | Tissues that contribute to ectopic prothoracic wing formation in *Blattella germanica*

As mentioned, wing serial homologs have been previously identified in the T1 of cockroaches through the analysis of the tissues that contribute to ectopic wing upon Hox reduction, both from homeotic mutants with ectopic T1 wings (*Prowing*) (Ross, 1964) and from ectopic wings produced by the postembryonic knockdown of *Scr* via RNAi (Elias-Neto & Belles, 2016; Hrycaj et al., 2010). We decided to revisit *Bg-Scr* knockdown in *B. germanica* using a modified RNAi protocol (scheme (ii), blue box in Figure S1), as this injection protocol appears to induce a more robust knockdown compared to other protocols.

Bg-Scr knockdown via the modified injection protocol produced adults with large ectopic T1 wings (Figures 3a,b, S4a, and S6a,b), suggesting that this transformation is stronger than the cases presented in previous studies (Figure S8) (Elias-Neto & Belles, 2016; Hrycaj et al., 2010; Ross, 1964). The lateral edge of the dorsal tergum is clearly contributing to the formation of the ectopic T1 wing in this transformation (arrow in Figures 3b, S4a,c, and S6b), an outcome consistent with previous studies (Elias-Neto & Belles, 2016; Hrycaj et al., 2010; Ross, 1964). The production of ectopic wings on T1 upon *Scr* reduction is a result of whole segment transformation, as we also observed a variety of traits besides ectopic wings that are indicative of T1-to-T2 transformation in the *Bg-Scr* RNAi individuals (Figures 3c–c″, S4b–b″, and S5c–c″). These include the appearance of a

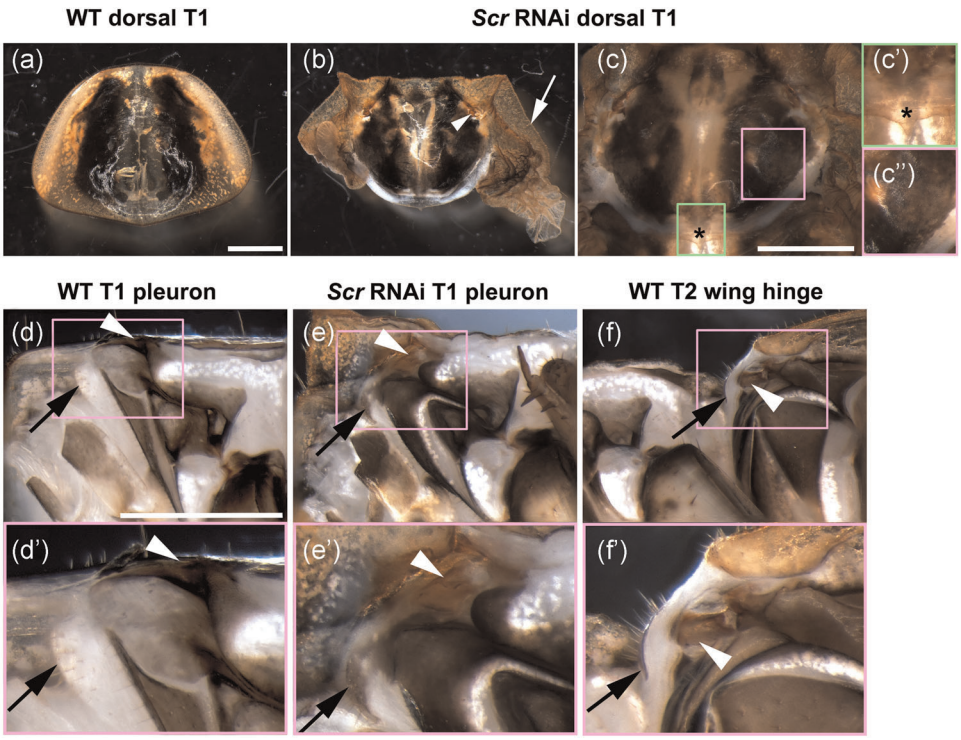

FIGURE 3 Contribution of T1 pleural plates to ectopic wing formation upon Hox reduction in *Blattella germanica*. (a–c″) Dorsal T1 of wild-type (a) and *Bg-Scr* RNAi (b–c″) individuals. c′ and c″ correspond to the areas outlined by green and pink boxes in c, respectively. (d–e′) T1 pleural region of wild-type (d–d′) and *Bg-Scr* RNAi (e–e′). (f–f′) lateral view of wild-type T2 wing hinge. d, e′, and f′ correspond to the area outlined by pink box in d, e, and f, respectively. Indicators are as follows: white arrow (ectopic T1 wing), Arrowhead (b, dorsal view of ectopic wing hinge, d–d′, T1 pleural plate, e–e′, ectopic wing hinge, and f–f′, wing hinge), pink box in c (sensory patch, c″), * (ectopic T1 scutellum), black arrow (d–d′, sensory patch, e–e′, ectopic wing sensory patch, and f–f′ wing sensory patch). Scale bars are 1 mm. Scale bar in a applies to b, and scale bar in d applies to e and f [Color figure can be viewed at wileyonlinelibrary.com]

sensory patch on the dorsal T1 surface (Figure 3c, c″, S4b,b″, and S6c,c″) that is normally found on the dorsal surface of T2 (Figure 2j,j″,k,k″), the transformation of the posterior T1 tergal edge into the posterior T2 tergal edge as noted by the presence of scutellum (* in Figures 3c–c′, S4b–b′, and S6c–c′), and similarity in pigmentation between T1 and T2 dorsal terga (Figure S4c).

In addition to the tergal edge of T1, Elias-Neto and Belles (2016) identified a region of the T1 pleuron that also contributes to ectopic wing upon *Bg-Scr* reduction, leading the authors to conclude that there are both tergal and pleural wing serial homologs in T1 of *B. germanica*. With this previous finding in mind, we analyzed the T1 pleural structures in detail. The *B. germanica* T1 pleuron consists of multiple intricately arranged plates (Figure 3d). In addition to the plate previously described (epimeron), we found a plate extremely dorsal within the pleural region that abuts the ventral edge of the tergum (arrowhead in Figures 3d–d′ and S6d–d′). Although this plate is extremely dorsal, it appears to still be a pleural plate as it is distinct from the tergum and is not associated with the sternum (Snodgrass, 1935b). Intriguingly, upon *Bg-Scr* reduction, this plate is transformed into a structure that resembles a portion of the T2 wing hinge (arrowhead in Figures 3b,e–f′, S4d–d′, and S6b,e–f′; Guthrie & Tindall, 1968). Furthermore, both the relative position of this transformed plate to other pleural structures and the change in pigmentation of this plate from black to light brown are also consistent with the transformation of this structure to a portion of the T2 wing hinge (Figures 3b,e–f′ and S6b,e–f′). Anterior to this plate in T1 is another structure that seems to be transforming into a portion of the T2 wing hinge (black arrow in Figures 3f–f′ and S6f–f′). In the wild-type T1, this structure is unpigmented and possesses short sensory hairs (Figures 3d–d′ and S6d–d′). Upon *Bg-Scr* RNAi, this structure becomes pigmented and the sensory hairs appear longer (Figures 3e–e′ and S6e–e′), resembling an anterior portion of the T2 wing hinge (black arrow in Figures 3f–f′ and S6f–f′). Together, these outcomes suggest that there are two previously unidentified regions of the T1 pleuron in *B. germanica* that appear to be transforming into wings (more specifically, the wing hinge) upon knockdown of *Bg-Scr*.

We were also curious about *Prowing*, the classic homeotic mutant that possesses ectopic wing tissues in T1 (Figure S8a; Ross, 1964; Tanaka & Ito, 1997). We could not find any existing stocks of living *Prowing* mutants; however, we were fortunate to be able to obtain several ethanol-preserved specimens of this mutant from Dr. Donald Mullins at Virginia Tech. Previous analysis of this mutant identified the tergal edge as the tissue that forms the ectopic wing (Ross, 1964). We confirmed this transformation in the specimen we received, which possessed small ectopic wing tissue originating from the lateral edge of the dorsal tergum (arrow in Figure S8a). In contrast, we could not detect transformation of the T1 pleural plates to wing hinge structures in the *Prowing* mutant (Figure S8b–b′), likely due to the weak nature of the transformation in this specimen. We also could not detect other indicators of transformation of T1 to T2, such as ectopic scutellum and sensory patch. Therefore, the *Prowing* phenotype appears to correspond to weak *Bg-Scr* RNAi transformation, in which only small ectopic wings are formed predominantly from the lateral terga.

In summary, our analyses of the strong T1-to-T2 transformation obtained through the improved *Scr* RNAi protocol has revealed that, in addition to the lateral tergum, multiple components of the T1 pleuron contribute to the formation of ectopic wing upon *Bg-Scr* reduction, even though we did not detect *vg*-dependency of these tissues in our *Bg-vg* RNAi analysis.

4 | DISCUSSION

4.1 | Tergal and pleural tissues that are potentially serially homologous to wings in *Blattella germanica*

Previous investigations into the wing-related structures in the wingless T1 segment of cockroaches have yielded varying conclusions as to the origin of insect wings, with some supporting a solely tergal origin (Hrycaj et al., 2010; Ross, 1964) and another supporting a dual origin (implicating both tergal and pleural tissues) (Elias-Neto & Belles, 2016). These previous studies in cockroaches identified potential wing serial homologs via the analysis of the tissues that transform into ectopic wings upon homeotic transformation of T1 and, in this way, limited our understanding of cockroach wing serial homologs to the T1 segment. In this study, we aimed to build upon the previous knowledge of wing serial homologs in cockroaches, specifically *B. germanica*, by both expanding the search for wing-related tissues outside of T1 through functional and expression analyses of *Bg-vg* and revisiting the T1 transformation induced by *Bg-Scr* knockdown with an improved RNAi scheme. Through our analysis of tissues dependent on the critical wing gene, *vg*, we were able to identify that the edge of the dorsal terga throughout thorax and abdomen is dependent on *Bg-vg* (Figure 4a, also see Figures 2 and S5). We also identified a *Bg-vg* dependent sclerotized plate in the abdominal segments that appears to be pleural in nature (Figure 4a, also see Figures 2h–i′, S5k–l′, and S7d–d′).

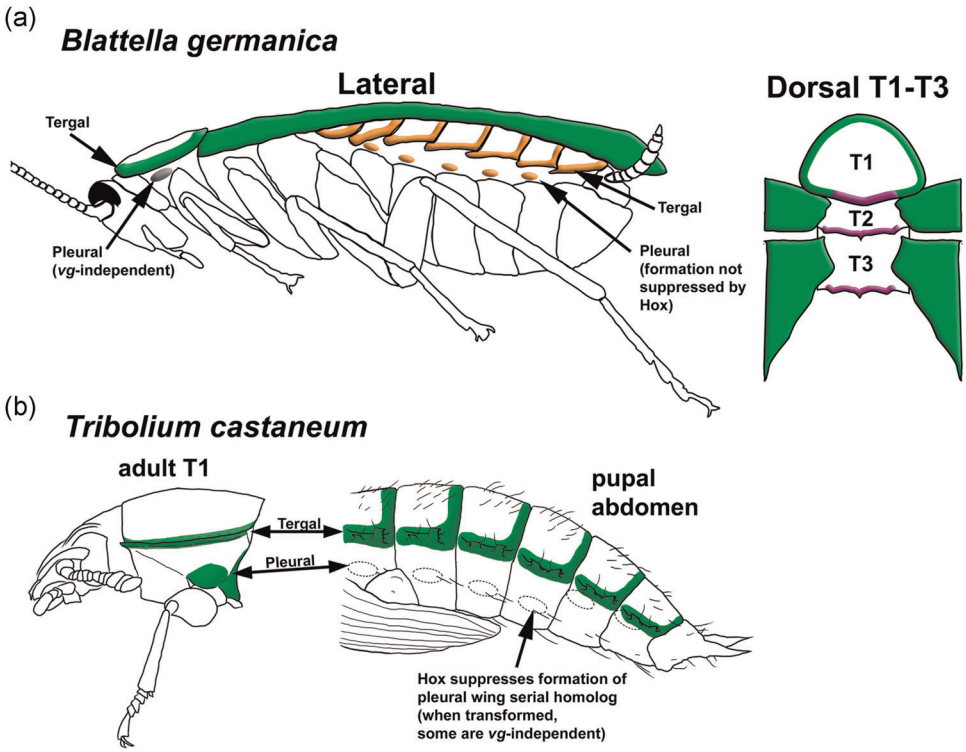

FIGURE 4 The wing serial homologs of *Blattella germanica* and *Tribolium castaneum*. (a) Possible wing serial homologs of *B. germanica*. *B. germanica* possesses two distinct sets of tissues that might be serially homologous to wings, one tergal and one pleural, in the wingless segments. In T1, the tergal edge is *vg*-dependent and transforms into wings upon Hox reduction, indicating that the tergal edge is a wing serial homolog (green). In addition, several pleural plates in T1 contribute to the formation of wings upon Hox transformation, suggesting that these plates might also be serially homologous to wings. However, these pleural pates are *vg*-independent, at least during the nymphal stage (gray). In contrast, the posterior portion of the tergal edge in the thoracic segments (i.e., scutellum) is *vg*-dependent, but does not contribute to wing formation (purple in dorsal view), suggesting that these tissues are not serially homologous to wings despite their *vg* dependency. In addition to these thoracic wing-related tissues, both tergal and pleural *vg*-dependent tissues are found in the abdominal segments (orange). These *vg*-dependent tissues are strong candidates for abdominal wing serial homologs in *B. germanica*; however, whether they could transform into wings upon Hox reduction is yet to be investigated. (b) The wing serial homologs of *T. castaneum* (green, adapted from Linz & Tomoyasu, 2018). *T. castaneum* possesses two distinct wing serial homologs in the wingless segments. However, the formation of pleural wing serial homologs in the abdomen is normally suppressed by Hox. In addition, some of the pleural wing serial homologs in the abdomen appear to be *vg*-independent [Color figure can be viewed at wileyonlinelibrary.com]

Upon revisiting the *Bg-Scr* knockdown using a modified RNAi protocol, we confirmed the finding from previous studies in cockroaches that the edge of the dorsal tergum contributes to ectopic wing formation (Elias-Neto & Belles, 2016; Hrycaj et al., 2010; Ross, 1964; Figure 4a, also see Figures 3b, S4a, and S6b). In addition, we identified two new regions of the T1 pleuron that transform into ectopic wing hinge structures upon reduction of *Bg-Scr* (Figure 4a, also see Figures 3d–f′ and S6d–f′). Combined, our analyses for *Bg-vg* and *Bg-Scr* provide an intriguing view of the tissues in *B. germanica* that are potentially serially homologous to wings (Figure 4a). It appears that, in the wingless segments (both T1 and abdomen), there are two distinct sets of tissues that satisfy at least one of the two criteria to be a wing serial homolog (i.e., dependency on wing genes and the capability to transform into wings upon homeotic transformation). If both of these tergal and pleural tissues are wing serial homologs, this outcome would further support to a dual origin of insect wings. However, the presence of a possible *vg*-independent tissue that contributes to wing formation upon homeotic transformation (gray in Figure 4a) and *vg*-dependent tissues that do not appear to contribute to wings (purple in Figure 4a) could complicate our interpretation of what wing serial homologs are, requiring us to investigate further into the complex evolutionary history of the tissues that contributed to the formation of insect wings.

4.2 | The T1 wing serial homologs of *Blattella germanica*

As mentioned, we have been using two criteria to identify wing serial homologs from wingless segments: the functional dependency on wing genes and the capability

to transform into wing upon homeotic transformation (Tomoyasu et al., 2017). The lateral edge of the dorsal T1 tergum in *B. germanica* is *Bg-vg* dependent (Figures 2, S2, S5, and S7; Table 1) and transforms into wing upon *Bg-Scr* reduction (Figures 3, S4, and S6; also reported in Elias-Neto & Belles, 2016). Therefore, this tissue fits both of the criteria to be considered a wing serial homolog (green in Figure 4a). But what about the pleural structures in T1 that have the ability to contribute to ectopic wings? To our surprise, we found that both of the pleural structures we identified as transforming into wing hinge are unaffected in *Bg-vg* RNAi (gray in Figures 4a and S9). There are several possible explanations for the *Bg-vg* RNAi insensitive nature of these T1 pleural plates in *B. germanica*. The first possibility, which is the most straight-forward interpretation of the outcome, is that the development of T1 pleural plates does not depend on the function of *Bg-vg*. The second possibility is related to the timing of RNAi. Unlike holometabolous insects, most of the body wall structures in hemimetabolous insects are formed during embryogenesis and the first instar nymphs already possess versions of these structures at the time of hatching that is very similar to those of adults. Therefore, knocking down *vg* during nymphal stages might have been too late to interfere with the development of some body wall structures. We attempted parental RNAi to circumvent the timing issue, but the efficiency of parental RNAi was extremely low (two individuals showed *Bg-vg* RNAi phenotypes out of >250 total nymphs, data not shown) leaving us unable to determine the *Bg-vg* dependency of the T1 pleuron in *B. germanica*. The third possibility, which is related to the second, is regarding the efficiency of *Bg-vg* RNAi in *B. germanica*, which might not have been sufficient to reveal all *vg*-dependent tissues in this species.

If either the second or third possibility (or both) is the case, the T1 pleural plates we identified could still satisfy the two criteria for wing serial homologs. Our expression analysis identified a *Bg-vg* expressing cell population ventral to the spiracle during embryogenesis (Figure 1g–g′; Supporting Information Movies S2 and S3). It is intriguing to speculate that this ventral *Bg-vg* expressing cell population corresponds to the pleural plates that transform into wings upon *Bg-Scr* RNAi. Although currently technically challenging, detailed expression analysis for *Bg-vg* during later embryogenesis as well as during nymphal development will help us further evaluate the *vg*-dependency of the T1 pleural plates.

What if the first possibility is the case and the pleural plates we identified are indeed independent of *Bg-vg* function? Are these structures still considered wing serial homologs in T1? We think they might be, based on their ability to contribute to wing formation upon homeotic transformation. Interesting insight comes from our investigation of wing serial homologs in the *T. castaneum* abdomen (Linz & Tomoyasu, 2018). When ectopic wing is induced in the abdomen of *T. castaneum* via Hox RNAi, a pleural population of cells starts to express *nubbin (nub*, another crucial wing gene (Cifuentes & Garcia-Bellido, 1997; Medved et al., 2015; Ng et al., 1995; Tomoyasu et al., 2009)), suggesting that these cells are gaining wing identity. In this context, some of these *nub*-positive pleural cells are found to be *vg*-independent (Linz & Tomoyasu, 2018), which might imply that *vg*-independent pleural wing serial homologs may not be limited to *B. germanica* T1. This *vg*-independent aspect of pleural wing serial homologs might be due to the nature of the structures they are transforming into. Upon *Bg-Scr* RNAi, the pleural structures we identified appear to be transforming into the wing hinge structure, which is, at least in some insects such as *D. melanogaster* and *T. castaneum*, outside of the functional domain of *vg* (but still within a part of the wing program, as evident from *nub* expression; Azpiazu & Morata, 2000; Clark-Hachtel et al., 2013; Linz & Tomoyasu, 2018; Tomoyasu et al., 2009).

The contribution of pleural plates to the formation of wings in cockroaches described here could also impact the recent challenge to the dual origin model put forward by Bruce and Patel (Bruce & Patel, 2020; also see Smith & Jockusch, 2020). The challenge is in part based on the authors' interpretation of our results presented in 2013 that the tergal and pleural tissues in the *Tribolium* T1 appear to merge along an anterior-posterior (AP) axis, rather than along a dorsal-ventral (DV) axis (Clark-Hachtel et al., 2013). More recently, we have shown that the merger of the two tissues in *Tribolium* could also happen along the DV axis in T1 (Clark-Hachtel et al., 2018), and more clearly in the abdominal segments (Linz & Tomoyasu, 2018). In the current report, we demonstrated that the merger of the T1 pleural tissues to form the ectopic wing also happens along the DV axis in *B. germanica* (Figure 3). Therefore, the discussion on the axis of merger for these two tissues can actually be used to support a dual origin model. Nonetheless, it will be crucial to further investigate the contribution of pleural plates to the formation of wings, not only upon homeotic transformation, but also during normal wing development in T2 and T3. In addition, investigating the dependency of the T1 *Bg-vg* independent pleural plates on other critical wing genes, such as *apterous* (*ap*) and *nub*, as well as the dependency of these tissues on other genes required for wing hinge development, will be helpful to understand the degree of genetic overlap between these

structures and wings. Collectively, these analyses will shed further light on the specific contribution of pleural plates to the evolution of insect wings.

4.3 | The incomplete nature of T1 transformation in hemimetabolous insects

In general, T1-to-T2 transformation induced by *Scr* RNAi is incomplete in hemimetabolous insects relative to the transformation that can be obtained in holometabolous insects (Elias-Neto & Belles, 2016; Hrycaj et al., 2010; Medved et al., 2015; Tomoyasu et al., 2005). For example, *Scr* RNAi in *T. castaneum*, a holometabolous insect, induces nearly complete transformation of T1 to T2, including the formation of fully hinged wings (Tomoyasu et al., 2005). In contrast, in *B. germanica*, although we see some wing hinge formation in our *Bg-Scr* RNAi individuals, the ectopic T1 wings are never fully hinged (Figures 3, S4, and S6). This is also the case for *Scr* transformation in other hemimetabolous insects, such as *Oncopeltus fasciatus* and another cockroach, *P. americana* (Hrycaj et al., 2010; Medved et al., 2015). In addition, the ectopic wings produced by *Scr* RNAi in hemimetabolous insects are usually much smaller than their normal T2 wings (Figures 3, S4, and S6; Elias-Neto & Belles, 2016; Hrycaj et al., 2010; Medved et al., 2015). Based on the outcome of their transcriptional analysis in *O. fasciatus*, Medved et al. (2015) proposed that the incomplete nature of the T1 ectopic wing could be attributed to the lack of the contribution from ventral components. As mentioned, many of the body wall components, including pleuron, are formed during embryogenesis and are well established before induction of transformation via postembryonic RNAi. Therefore, it is possible that the inability to obtain a large, hinged ectopic wing in hemimetabolous insects stems from the difficulty to recruit pleural components to the formation of this wing through postembryonic knockdown. As proposed by Medved et al. (2015), this inability of the pleural components to join the *Scr* RNAi-induced ectopic wings in hemimetabolous insects might be a reflection of a more ancestral state of the insect prothorax, which may point toward a step-wise evolution of insect wings, that is, an initial hinge-less tergal-derived winglet followed by a more complete wing through the joining of pleural components. However, the fact that we could obtain an *Scr*-RNAi induced transformation stronger than those previously reported through improved RNAi protocols might suggest that the incomplete nature of the transformation could, in part, be attributed to a technical difficulty. Although technically challenging, knocking down or knocking out *Scr* throughout *B. germanica* development, including during embryogenesis, may give us more insight into the incomplete nature of homeotic transformation in hemimetabolous insects, which in turn can help further our understanding of how insect wings emerged.

4.4 | On abdominal wing serial homologs in insects

Although markedly less work has been done to identify wing serial homologs in the abdominal segments of insects, previous studies have identified wing-related structures in the abdomen of some insects (Hu et al., 2018; Linz & Tomoyasu, 2018; Ohde et al., 2013). Ohde et al. found that the defensive structures in the pupal abdomen of *Tenebrio molitor*, called gin-traps, are also *vg*-dependent and that these structures transform into wings upon Hox reduction. These outcomes led the authors to propose that the gin-traps, a tergal structure, are wing serial homologs in the abdominal segments of beetles (Ohde et al., 2013). Through detailed Hox transformation analyses, Linz and Tomoyasu found that, in addition to the gin-trap cells, a separate population of cells in the pleural region appears upon Hox reduction and transforms into tissues with wing identity in the abdominal segment of *T. castaneum*. The latter study suggests an interesting situation for the state of wing serial homologs in the beetle abdomen, where, under normal Hox function, only one type of wing serial homolog is present (the gin-traps, tergal wing serial homolog; Figure 4b). Upon Hox reduction, a second wing serial homolog in the pleural region appears and merges with the tergal wing serial homolog to form an ectopic wing.

In the abdominal segments of *B. germanica*, we identified two distinct sets of *vg*-dependent tissues, the edge of the tergum and a pleural plate (orange in Figure 4a, also see Figures 2, S5, and S7). Considering the parallel situation of *vg*-dependent tissues in T1 and the beetle abdomen, both of these tissues in the *B. germanica* abdomen could be serially homologous to wings (Figure 4). However, it is yet to be determined how these tergal and pleural abdominal wing serial homologs contribute to an ectopic wing upon removal of Hox function in the abdomen of *B. germanica*.

There are several additional tissues in the insect abdomen that have been traditionally viewed as potential wing serial homologs, including the abdominal gill of mayflies and the stylus of bristletails (reviewed in Clark-Hachtel & Tomoyasu, 2016). Niwa et al. (2010) found that some wing genes are indeed expressed in these tissues. More recently, Almudi et al. (2020) demonstrated a large overlap in the transcriptome of wings and

abdominal gills in the mayfly *Cloeon dipterum*. The developmental origin of these abdominal tissues (specifically whether they are of tergal or pleural origin) and their Hox regulation have yet to be explored. Therefore, further investigation into abdominal wing serial homologs in various insects will inform our understanding of the plesiomorphic state (i.e., represents ancestral morphology) of the abdominal pleural wing serial homologs and the evolution of wing related tissues.

4.5 | *vg*-dependent tissues and wing serial homologs

In *B. germanica*, we saw two interesting cases of discrepancy between the *vg*-dependent tissues and the tissues that can contribute to ectopic wing formation. As discussed above, the pleural plates in T1 are the first case, where these plates transform into wings upon *Scr* RNAi but are independent of *vg*-function, at least during the nymphal stage (gray in Figure 4a). In addition, we found that the scutellum of T2 and T3, a structure at the posterior edge of the tergum, is *Bg-vg* dependent (Figures 2j–j′,k–k′ and S5i–i′,j–j′), even though the scutellum is not directly related to wings. The latter discrepancy indicates that not all *vg*-dependent tergal tissues are serially homologous to wings, which signifies the importance of using multiple measures when identifying wing serial homologs, including the ability of the structure to contribute to ectopic wings and the degree of genetic overlap, beyond just *vg*, between the structure of interest and wings.

The presence of non-wing *vg*-dependent tergal tissues is not limited to cockroaches. Previously, Medved et al. (2015) found that the scutellum of winged segments of *O. fasciatus* is also *vg*-dependent, even though the scutellum in this insect is not dependent on other wing genes, such as *nub*. In the *T. castaneum* abdomen, we found that some of the *vg*-expressing cells along the posterior edge of the tergum do not contribute to ectopic wing and lack dependency on other wing gene network components, such as *ap* and Wingless signal, both of which function in the lateral tergum (during gin-trap formation; Linz & Tomoyasu, 2018). These results are in line with our current study in *B. germanica* and suggest that there are two populations of *vg*-dependent tissues even within the tergum; the posteriorly located tissues that are not related to wings and the laterally located tissues that are serially homologous to wings.

The identification of wing-related structures in the wingless segments of insects and of non-winged arthropods using evo-devo approaches now covers a wide swath of the arthropod phylogenetic tree including crustaceans (Averof & Cohen, 1997; Clark-Hachtel & Tomoyasu, 2020), non-winged insects (Niwa et al., 2010), hemimetabolous insects (this study and (Elias-Neto & Belles, 2016; Hrycaj et al., 2010; Medved et al., 2015; Niwa et al., 2010)), and holometabolous insects (Clark-Hachtel et al., 2013, 2018; Hu et al., 2018; Linz & Tomoyasu, 2018; Ohde et al., 2013). These studies have provided a wealth of intriguing insights into the evolutionary origin of insect wings. Future investigations into the detailed molecular and developmental mechanisms operating in these wing-related tissues will enable us to identify the unique mechanisms in the winged segments that have facilitated the evolution of insect wings.

4.6 | Re-evaluating the concept of wing serial homologs

Traditionally, the identification of tissues in the wingless segments that are serially homologous to wings has been the main approach to gain insights into the evolutionary origin of insect wings. Only a handful of non-wing tissues were identified as wing serial homologs through classic morphological analyses because of the drastic morphological difference between wings and other serially homologous tissues. However, through recent evo-devo studies, we came to realize that wing serial homologs are not unique structures, and instead that there are tissues evolutionarily related to wings in almost every wingless trunk segment (i.e., T1 and abdominal segments) of many insects. It is now clear that these tissues in the wingless segments represent a more ancestral state in evolution, while the wing represents the most derived (i.e., an apomorphic) condition. This realization makes the term "wing serial homologs" difficult to use, as this group of tissues is currently named after the most extensively modified and evolutionarily unique member of the group. Instead, it is easier to define these tissues based on their ancestral identity, as in "tergal serial homologs" and "pleural serial homologs" (see Tomoyasu et al., 2017, for a more detailed discussion). In the dual origin model, the wing is considered an overlap between these two groups of serial homologs, namely the "tergal-pleural serial homolog." In this report, we continued to use the term "wing serial homolog", since this phrase has been used for centuries and is widely accepted in the field. However, the phrases "tergal serial homolog" and "pleural serial homolog" will be useful when further dissecting the tissues that have contributed to the evolution of insect wings.

ACKNOWLEDGMENTS

The authors thank Donald Mullins and Sandra Gabbert at Virginia Tech for providing samples of *B. germanica* mutant

strains, and the Center for Advanced Microscopy and Imaging (CAMI) at Miami University for technical support. The authors acknowledge and thank the staff (Dr. Andor Kiss and Ms. Xiaoyun Deng) of the Center for Bioinformatics & Functional Genomics (CBFG) at Miami University for instrumentation and computational support. The authors also thank Shuxia Yi and Ferran Borràs-Castells for technical assistance, Takahiro Ohde for helpful comments, and members of the Tomoyasu lab for helpful discussion. This study is supported by the Miami University Faculty Research Grants Program (CFR; to Yoshinori Tomoyasu), the National Science Foundation (NSF; IOS1557936 to Yoshinori Tomoyasu), an NSF Graduate Research Fellowship (to Courtney Clark-Hachtel), the Spanish Ministry of Economy and Competitiveness (including support for the visit of Ana Fernandez-Nicolas to the Tomoyasu lab; CGL2012-36251, CGL2015-64727-P, and PID2019-104483GB-I00 to Xavier Belles), the Catalan Government (2014 SGR 619, 2017 SGR 10c0 to Xavier Belles), and European Fund for Economic and Regional Development (FEDER funds to Xavier Belles).

CONFLICT OF INTERESTS

The authors declare that there are no conflict of interests.

DATA AVAILABILITY STATEMENT

The sequences of the cDNA fragments cloned in this study have been deposited in GenBank with the accession numbers MN337883 (*Bg-vg*) and MN337884 (*Bg-Scr*).

ORCID

Courtney Clark-Hachtel https://orcid.org/0000-0003-0783-3534
Ana Fernandez-Nicolas https://orcid.org/0000-0002-4570-1893
Xavier Belles http://orcid.org/0000-0002-1566-303X
Yoshinori Tomoyasu http://orcid.org/0000-0001-9824-3454

REFERENCES

Almudi, I., Vizueta, J., Wyatt, C. D. R., de Mendoza, A., Marlétaz, F., Firbas, P. N., Feuda, R., Masiero, G., Medina, P., Alcaina-Caro, A., Cruz, F., Gómez-Garrido, J., Gut, M., Alioto, T. S., Vargas-Chavez, C., Davie, K., Misof, B., González, J., Aerts, S., … Casares, F. (2020). Genomic adaptations to aquatic and aerial life in mayflies and the origin of insect wings. *Nature Communications*, *11*, 2631.

Angelini, D. R., & Kaufman, T. C. (2005). Comparative developmental genetics and the evolution of arthropod body plans. *Annual Review of Genetics*, *39*, 95–119.

Averof, M., & Cohen, S. M. (1997). Evolutionary origin of insect wings from ancestral gills. *Nature*, *385*, 627–630.

Azpiazu, N., & Morata, G. (2000). Function and regulation of *homothorax* in the wing imaginal disc of *Drosophila*. *Development*, *127*, 2685–2693.

Baena-López, L. A., & García-Bellido, A. (2003). Genetic requirements of *vestigial* in the regulation of *Drosophila* wing development. *Development*, *130*, 197–208.

Bernard, F., Lalouette, A., Gullaud, M., Jeantet, A. Y., Cossard, R., Zider, A., Ferveur, J. F., & Silber, J. (2003). Control of *apterous* by *vestigial* drives indirect flight muscle development in *Drosophila*. *Developmental Biology*, *260*, 391–403.

Bruce, H. S., & Patel, N. H. (2020). Knockout of crustacean leg patterning genes suggests that insect wings and body walls evolved from ancient leg segments. *Nature Ecology and Evolution*, *4*, 1703–1712.

Cifuentes, F. J., & Garcia-Bellido, A. (1997). Proximo-distal specification in the wing disc of *Drosophila* by the nubbin gene. *Proceedings of the National Academy of Sciences of the United States of America*, *94*, 11405–11410.

Clark-Hachtel, C. M., Linz, D. M., & Tomoyasu, Y. (2013). Insights into insect wing origin provided by functional analysis of *vestigial* in the red flour beetle, *Tribolium castaneum*. *Proceedings of the National Academy of Sciences of the United States of America*, *110*, 16951–16956.

Clark-Hachtel, C. M., Moe, M. R., & Tomoyasu, Y. (2018). Detailed analysis of the prothoracic tissues transforming into wings in the *Cephalothorax* mutants of *Tribolium*. *Arthropod Structure & Development*, *47*, 352–361.

Clark-Hachtel, C. M., & Tomoyasu, Y. (2016). Exploring the origin of insect wings from an evo-devo perspective. *Current Opinion in Insect Science*, *13*, 77–85.

Clark-Hachtel, C. M., & Tomoyasu, Y. (2020). Two sets of candidate crustacean wing homologues and their implication for the origin of insect wings. *Nature Ecology and Evolution*, *4*, 1694–1702.

Deng, H., Bell, J. B., & Simmonds, A. J. (2010). Vestigial is required during late-stage muscle differentiation in *Drosophila melanogaster* embryos. *Molecular Biology of the Cell*, *21*, 3304–3316.

Deng, H., Hughes, S. C., Bell, J. B., & Simmonds, A. J. (2009). Alternative requirements for Vestigial, Scalloped, and Dmef2 during muscle differentiation in *Drosophila melanogaster*. *Molecular Biology of the Cell*, *20*, 256–269.

Elias-Neto, M., & Belles, X. (2016). Tergal and pleural structures contribute to the formation of ectopic prothoracic wings in cockroaches. *Royal Society Open Science*, *3*, 160347.

Guthrie, D. M., & Tindall, A. R. (1968). The exoskeleton, *The biology of the cockroach* (pp. 23–60). Edward Arnold Publisher.

Halder, G., Polaczyk, P., Kraus, M. E., Hudson, A., Kim, J., Laughon, A., & Carroll, S. (1998). The Vestigial and Scalloped proteins act together to directly regulate wing-specific gene expression in *Drosophila*. *Genes and Development*, *12*, 3900–3909.

Hrycaj, S., Chesebro, J., & Popadić, A. (2010). Functional analysis of *Scr* during embryonic and post-embryonic development in the cockroach, *Periplaneta americana*. *Developmental Biology*, *341*, 324–334.

Hu, Y., Schmitt-Engel, C., Schwirz, J., Stroehlein, N., Richter, T., Majumdar, U., & Bucher, G. (2018). A morphological novelty evolved by co-option of a reduced gene regulatory network

and gene recruitment in a beetle. *Proceedings of the Royal Society B: Biological Sciences*, *285*, 20181373.

Hughes, C. L., & Kaufman, T. C. (2002). Hox genes and the evolution of the arthropod body plan. *Evolution & Development*, *4*, 459–499.

Kim, J., Sebring, A., Esch, J. J., Kraus, M. E., Vorwerk, K., Magee, J., & Carroll, S. B. (1996). Integration of positional signals and regulation of wing formation and identity by *Drosophila vestigial* gene. *Nature*, *382*, 133–138.

Kukalova-Peck, J. (1983). Origin of the insect wing and wing articulation from the arthropodan leg. *Canadian Journal of Zoology*, *61*, 1618–1669.

Linz, D. M., Clark-Hachtel, C. M., Borràs-Castells, F., & Tomoyasu, Y. (2014). Larval RNA interference in the red flour beetle, *Tribolium castaneum*. *Journal of Visualized Experiments*, e52059.

Linz, D. M., & Tomoyasu, Y. (2018). Dual evolutionary origin of insect wings supported by an investigation of the abdominal wing serial homologs in *Tribolium*. *Proceedings of the National Academy of Sciences of the United States of America*, *115*, E658–E667.

Maestro, J. L., Pascual, N., Treiblmayr, K., Lozano, J., & Bellés, X. (2010). Juvenile hormone and allatostatins in the German cockroach embryo. *Insect Biochemistry and Molecular Biology*, *40*, 660–665.

Mashimo, Y., & Machida, R. (2017). Embryological evidence substantiates the subcoxal theory on the origin of pleuron in insects. *Scientific Reports*, *7*, 12597.

Medved, V., Marden, J. H., Fescemyer, H. W., Der, J. P., Liu, J., Mahfooz, N., & Popadić, A. (2015). Origin and diversification of wings: Insights from a neopteran insect. *Proceedings of the National Academy of Sciences of the United States of America*, *112*, 15946–15951.

Nagaso, H., Murata, T., Day, N., & Yokoyama, K. K. (2001). Simultaneous detection of RNA and protein by in situ hybridization and immunological staining. *Journal of Histochemistry and Cytochemistry*, *49*, 1177–1182.

Ng, M., Diaz-Benjumea, F. J., & Cohen, S. M. (1995). *nubbin* encodes a POU-domain protein required for proximal-distal patterning in the *Drosophila* wing. *Development*, *121*, 589–599.

Niwa, N., Akimoto-Kato, A., Niimi, T., Tojo, K., Machida, R., & Hayashi, S. (2010). Evolutionary origin of the insect wing via integration of two developmental modules. *Evolution & Development*, *12*, 168–176.

Ohde, T., Yaginuma, T., & Niimi, T. (2013). Insect morphological diversification through the modification of wing serial homologs. *Science*, *340*, 495–498.

Pearson, J. C., Lemons, D., & McGinnis, W. (2005). Modulating Hox gene functions during animal body patterning. *Nature Reviews Genetics*, *6*, 893–904.

Philip, B. N., & Tomoyasu, Y. (2011). Gene knockdown analysis by double-stranded RNA injection. *Methods in Molecular Biology*, *772*, 471–497.

Piulachs, M. D., Pagone, V., & Bellés, X. (2010). Key roles of the *Broad-Complex* gene in insect embryogenesis. *Insect Biochemistry and Molecular Biology*, *40*, 468–475.

Prokop, J., Pecharová, M., Nel, A., Hörnschemeyer, T., Krzemińska, E., Krzemiński, W., & Engel, M. S. (2017). Paleozoic nymphal wing pads support dual model of insect wing origins. *Current Biology*, *27*, 263–269.

Quartau, J. A. (1986). An overview of the paranotal theory on the origin of the insect wings. Publicações do Instituto de Zoologia "Dr. Augusto Nobre" Fac. Ciencias Do Porto, 194, 1–42.

Rasnitsyn, A. P. (1981). A modified paranotal theory of insect wing origin. *Journal of Morphology*, *168*, 331–338.

Requena, D., Álvarez, J. A., Gabilondo, H., Loker, R., Mann, R. S., & Estella, C. (2017). Origins and specification of the *Drosophila* wing. *Current Biology*, *27*, 3826–3836.e5.

Rogers, B. T., Peterson, M. D., & Kaufman, T. C. (1997). Evolution of the insect body plan as revealed by the *Sex combs reduced* expression pattern. *Development*, *124*, 149–157.

Ross, M. H. (1964). Pronotal wings in *Blattella germanica* (L.) and their possible evolutionary significance. *American Midland Naturalist*, *71*, 161–180.

Shippy, T. D., Coleman, C. M., Tomoyasu, Y., & Brown, S. J. (2009). Concurrent *in situ* hybridization and antibody staining in red flour beetle (*Tribolium*) embryos. *Cold Spring Harbor Protocols, 4*, pdb.prot5257.

Smith, F. W., & Jockusch, E. L. (2020). Into the body wall and back out again. *Nature Ecology and Evolution, 4*, 1580–1581.

Snodgrass, R. E. (1935a). The abdomen, *Principles of insect morphology* (pp. 246–279). Cornell University Press.

Snodgrass, R. E. (1935b). The thorax, *Principles of insect morphology* (pp. 157–192). Cornell University Press.

Sánchez-Higueras, C., Sotillos, S., & Castelli-Gair Hombría, J. (2014). Common origin of insect trachea and endocrine organs from a segmentally repeated precursor. *Current Biology*, *24*, 76–81.

Tanaka, A., & Ito, T. (1997). Studies of the genetics and expression of Prowing (*Pw*): A primitive homeotic mutant of the German cockroach, *Blattella germanica*. *Zoological Science*, *14*, 339–346.

Tomoyasu, Y. (2018). Evo–devo: The double identity of insect wings. *Current Biology*, *28*, R75–R77.

Tomoyasu, Y., Arakane, Y., Kramer, K. J., & Denell, R. E. (2009). Repeated co-options of exoskeleton formation during wing-to-elytron evolution in beetles. *Current Biology*, *19*, 2057–2065.

Tomoyasu, Y., Ohde, T., & Clark-Hachtel, C. M. (2017). What serial homologs can tell us about the origin of insect wings. *F1000Research*, *6*, 268.

Tomoyasu, Y., Wheeler, S. R., & Denell, R. E. (2005). *Ultrabithorax* is required for membranous wing identity in the beetle *Tribolium castaneum*. *Nature*, *433*, 643–647.

Williams, J. A., Bell, J. B., & Carroll, S. B. (1991). Control of *Drosophila* wing and haltere development by the nuclear *vestigial* gene product. *Genes and Development*, *5*, 2481–2495.

SUPPORTING INFORMATION

Additional Supporting Information may be found online in the supporting information tab for this article.

How to cite this article: Clark-Hachtel C, Fernandez-Nicolas A, Belles X, Tomoyasu Y. Tergal and pleural wing-related tissues in the German cockroach and their implication to the evolutionary origin of insect wings. *Evolution & Development*. 2021;e12372.
https://doi.org/10.1111/ede.12372